

Modelling of the agglomeration of Ni-particles in anodes of solid oxide fuel cells

R. VAßEN, D. SIMWONIS, D. STÖVER

Institut für Werkstoffe und Verfahren der Energietechnik 1, Forschungszentrum Jülich, 52425 Jülich, Germany

E-mail: r.vassen@fz-juelich.de

The degradation of anodes of solid oxide fuel cells (SOFC), which consist of a porous metal - solid electrolyte material is described by a two particle model. The model is based on two main assumptions. Firstly, the difference in metal particle diameter is the driving force for the observed coarsening of the larger metal particle during long term annealing. Secondly, surface diffusion of metal atoms on the particle surface is the dominant diffusion mechanism. Additionally, a function was introduced which considers the limited space for the growth of the nickel particles in the cermet material. The found analytical function for the growth kinetics was compared to experimental results for the growth of nickel particles in a nickel - yttria stabilised zirconia (YSZ) anode annealed at 1000°C up to 4000 h. The model describes the time dependence of the observed particle radii in an adequate way. The resultant surface diffusion coefficients for Ni are lower than results found in literature. Possible explanations are discussed. However, the result shows that the proposed mechanism – surface diffusion of nickel atoms - is fast enough to explain the found amount of Ni agglomeration in SOFC anodes and is therefore considered to be the dominant mechanism. © 2001 Kluwer Academic Publishers

1. Introduction

In most SOFC concepts a porous cermet made of YSZ and Ni particles is used as anode material [1, 2]. The electrochemical performance of these anodes is depending on the number of so-called three phase boundaries, i.e. the lines, where pores (burning gas supply), solid electrolyte (O^{2-} supply) and metal (removal of electrons) are in contact. Often, a functional layer, which has the same composition as the anode substrate but a finer particle size distribution, is applied to the anode substrate to increase the electrochemical performance. During high temperature operation for long periods of time a degradation of the electrochemical performance has been observed [3, 4]. This degradation is mainly attributed to the Ni agglomeration and the corresponding reduction of the three phase boundaries. While in principle it is obvious that the Ni particle will grow during high temperature operation a detailed description of the kinetics of this process is difficult due to the complexity of the structure. Two types of materials (YSZ and Ni) and additionally pores exist in the structure with all of them having multi-modal size distributions.

An approach to describe the degradation was performed using a so called correlated percolation model, in which monosized particles are located on a face-centered cubic lattice [5, 6]. In the computer simulation sintering between two metal particles occurred instantaneously with a certain probability. The result is an unchanged particle and one pore or one dead particle

with no more electrochemical contribution to the network. The model gives an insight in the development of active bonds in the anode, the density of three phase boundaries and the transport resistance in anodic materials. However, a correlation of the introduced input parameters (e.g. sintering probability) with actual materials parameters like particle size, particle size distributions, or diffusion coefficients or experimentally found microstructural changes, e.g. Ni particle growth, is difficult. In the present paper a different approach was used. The problem was reduced to a two particle problem, i.e. two Ni particles of different sizes in contact with each other. Even this two particle problem is a rather complex one if analysed in detail. Pan *et al.* [7] studied the neck growth of two particles in contact by finite element calculations. The time of disappearance of the boundary t_d was derived from the simulation and could be described by an empirical formula. The major parameters which determine t_d are the surface diffusion coefficient (much more than the grain boundary diffusion coefficient) and the size of the particles. In the present study, only surface diffusion was taken into account to derive a kinetic equation for the Ni particle growth. This equation was compared to results of the finite element calculations.

Additionally, a term was introduced in the model, which takes into account the limited space for Ni particle growth within the cermet. The additional fitting factor of this term is closely related to the pore volume, which can be easily determined experimentally.

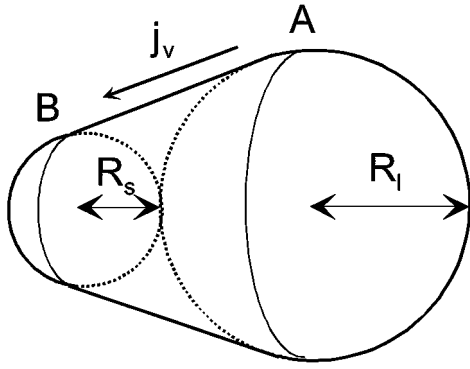


Figure 1 Geometry of the used two particle model.

2. Theory

The geometry of the used two particle system is shown in Fig. 1. This geometry implies that neck growth does not play a dominant role during particle growth. This assumption can be justified by that fact that the anode material was sintered during the manufacture of the SOFC at relatively high temperatures (typically 1400°C). As a result, neck growth should be finished or should not play an important role during operation at low temperatures (typically below 1000°C).

Using the geometry in Fig. 1 it is possible to derive a simple equation for the vacancy flow from the large to the small particle. The derivation is quite similar to the one used in sintering theory [8]. The difference in curvature between large and small particle leads to different pressures p in the matrix and hence different vacancy concentrations in the two particles. The difference in vacancy concentration ΔC is for values which are small compared to the vacancy concentration of a flat surface C_0 proportional to the change of free energy of vacancy formation ΔG :

$$\Delta C = C_0 \frac{\Delta G}{kT} = C_0 \frac{\Omega \Delta p}{kT} = C_0 \frac{\Omega \gamma_s \left(\frac{1}{r_s} - \frac{1}{r_l} \right)}{kT} \quad (1)$$

with Ω being the volume of a vacancy (\approx atomic volume), γ_s surface energy, k Boltzmann constant, and T temperature. The expression for the pressure implies, that the surface is curved only in one direction. This is true for the intermediate part of the geometry given in Fig. 1 (conical shape). The higher pressure at both ends arising from the higher curvature will not be considered because in an anode such free ends, e.g. particles without contact to the neighbouring particles, are rare.

The difference in vacancy concentration will lead to a vacancy flow j_v (or an atom flux in the opposite direction) from the large to the small particle according to Fick's law. In the case of surface diffusion this can be written as:

$$j_v = D_{v,s} \frac{dC}{dx} \approx D_{v,s} \frac{\Delta C}{\Delta x} = D_{v,s} \frac{C_0 \Omega \gamma_s}{\Delta x k T} \left(\frac{1}{r_l} - \frac{1}{r_s} \right) \quad (2)$$

with $D_{v,s}$ being the vacancy surface diffusion coefficient. The diffusion distance Δx from point A to B in

Fig. 2 is:

$$\Delta x = \sqrt{(r_l + r_s)^2 + (r_l - r_s)^2} \quad (3)$$

Before we calculate the growth rate of the large particle it is useful to introduce a mean particle radius r_m and a particle radius difference Δr :

$$r_m = (r_l + r_s)/2 \quad (4a)$$

and

$$\Delta r = r_l - r_s \quad (4b)$$

An important assumption in our model is that Δr is proportional to r_m for all times. This implies that the particle size distribution keeps a similar shape during growth. The proportionality constant between Δr and r_m is called β :

$$\Delta r = 2\beta r_m \quad (5)$$

This assumption is a basic one for the model because it determines the kinetics of the particle growth. An intuitive justification for the assumption is that it holds also for other important grow laws, like Ostwald ripening [9]. As discussed in the next section a more straight forward justification is the fact that the measured particle size distributions indeed showed this behaviour. Furthermore, it is found that the model derived in the following is not very sensitive to changes of the parameter β . A change of β of about 10% leads to a 1% change in particle radius.

We can now calculate the volume change per time (dV/dt) due to diffusion through a surface area with thickness δ_s and circumference $2\pi r_m$, which is in fact a kind of mean value:

$$\frac{dV}{dt} = -j_v \delta_s 2\pi r_m \Omega \quad (6)$$

This rate of volume change is equal to the rate of volume change (the growth) of the large particle:

$$\frac{dV}{dt} = 4\pi r_l^2 \frac{dr_l}{dt} \quad (7)$$

Using (2, 4–7) and $D_S = D_{v,s} C_0 \Omega$ for the atomic surface diffusion coefficient [10], we finally have:

$$\frac{dr_m}{dt} = \frac{\pi \delta_s \Omega D_s \gamma_s}{2kT r_m^3} \frac{\beta}{(1 - \beta^2)(1 + \beta)^3 \sqrt{1 + \beta^2}} \quad (8a)$$

or after integration with respect to time t :

$$r(t)_m^4 - r(0)_m^4 = \frac{2\delta_s \Omega D_s \gamma_s t}{kT} \frac{\beta}{(1 - \beta^2)(1 + \beta)^3 \sqrt{1 + \beta^2}} \quad (8b)$$

A comparison with the results from finite element calculation [7] of the two particle sintering will be made in the following. In this simulation, the time of disappearance of the grain boundary, e.g. the disappearance of the smaller particle, was empirically determined by

fitting the simulation results. The following formula was found:

$$t_d = \frac{kT}{\Omega\gamma_s D_s \delta_s} r_s^4 \left(\frac{D_s \delta_s}{D_{gb} \delta_{gb}} \right)^{0.15} \left(\frac{\gamma_{gb}}{\gamma_s} \right) \left(\frac{r_s}{r_1} \right)^{0.63} \quad (9)$$

A direct comparison with our model is not possible, because due to assumption (5) the particles will not disappear. However, we can calculate the time needed for a particle of the mean radius to growth up to the double volume:

$$\tilde{t}_d = \frac{kT}{\Omega\gamma_s D_s \delta_s} r_m^4 \left(\frac{2^{4/3} - 1}{2} \right) \times \left(\frac{(1 - \beta^2)(1 + \beta)^3 \sqrt{1 + \beta^2}}{\beta} \right) \quad (10)$$

The first terms in Equations 9 and 10 are equal and the terms in brackets differ not to much from unity. Hence, the results of our model are close to the ones of the more precise calculation.

The approach does not consider the limited space for growth within the cermet microstructure. To incorporate this into the model we introduce an additional term in (8) which will go to zero when the volume of the large particle reaches some maximal value $4/3\pi r_{\max}^3$:

$$\frac{r_{\max}^3 - r_1^3(t)}{r_{\max}^3 - r_1^3(0)} = \frac{1 - y(t)^3}{1 - y(0)^3} \quad \text{with} \quad y(t) = (1 + \beta) \frac{r_m(t)}{r_{\max}} \quad (11)$$

Using the new variable y we find the following equation for the growth rate of the mean particle diameter:

$$\frac{dy(t)}{dt} = \frac{\delta_s \Omega D_s \gamma_s}{2kT r_{\max}^4} \frac{1}{1 - y(0)^3} \frac{\beta(1 + \beta)}{(1 - \beta^2)\sqrt{1 + \beta^2}} \frac{1 - y(t)}{y(t)^3} \quad (12)$$

The solution is:

$$\begin{aligned} \frac{A}{r_{\max}^4} \frac{1}{1 - y(0)^3} \frac{\beta(1 + \beta)}{(1 - \beta^2)\sqrt{1 + \beta^2}} t \\ = -y - \frac{1}{6} \ln \left(\frac{(1 - y)^2}{1 + y + y^2} \right) \\ + \frac{1}{\sqrt{3}} \arctan \frac{2y + 1}{\sqrt{3}} + C \end{aligned} \quad (13)$$

with C being an integration constant determined by setting $t = 0$ in (13) and $A = (\delta_s \Omega D_s \gamma_s) / (2kT)$.

3. Comparison with experimental results

The Ni agglomeration was investigated in SOFC anodes which have been prepared by the Coat Mix process [11]. A typical microstructure is shown in Fig. 2. Particle size distributions have been determined from optical micrographs using image analysis techniques. The found results were multiplied by a factor of 1.5 to convert the 2 dimensional intercept length into a 3 dimensional particle size diameter [12]. Anodes have been annealed at 1000°C for up to 4000 hours in an Ar/4% H₂/4%

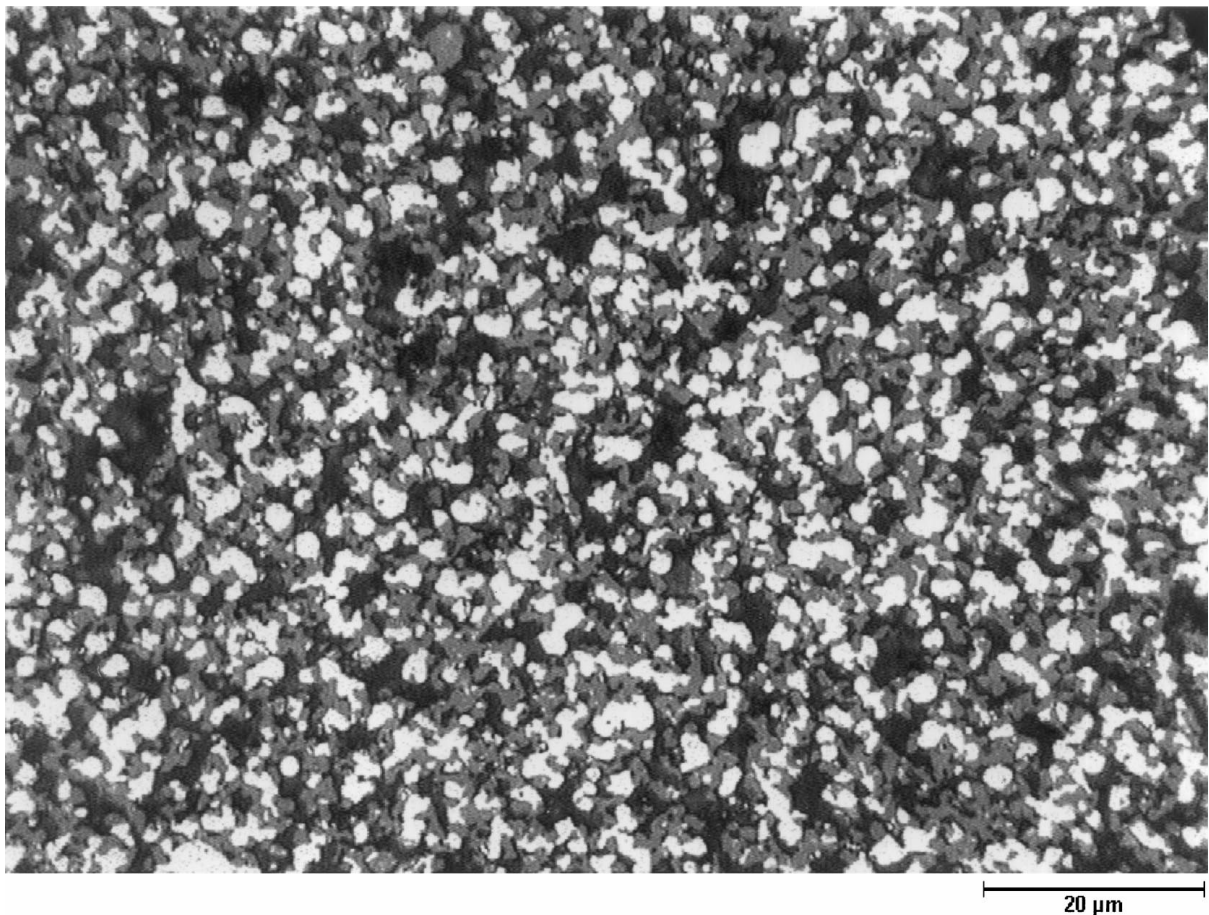


Figure 2 Microstructure of a SOFC anode prepared by the Coat Mix process [10]. Nickel appears white, YSZ grey and the pores are black.

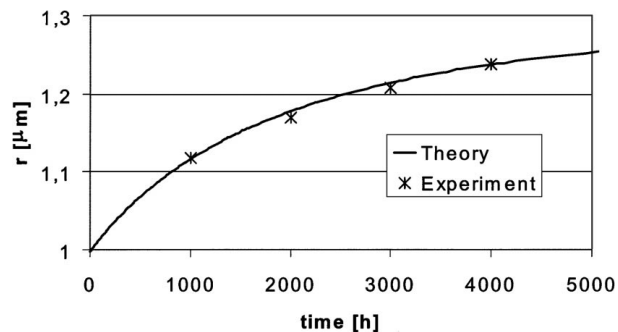


Figure 3 A fit of the theoretical growth law (13) for the mean particle radius compared to the experimental results for Ni particles in a SOFC anode annealed at 1000°C for the given times.

H₂O atmosphere to investigate the growth of the nickel particles. More details about the experimental procedure are found in [13].

A comparison of the experimental results with theory is given in Fig. 3. The growth law given in Equation 13 contains three free parameters: β , A and r_{\max} . β was determined from the particle size distributions giving approximately 0.75 ± 0.07 independent from annealing time. A and r_{\max} were used as fitting parameters. A good fit (Fig. 3) was obtained by $A = 8.5 \times 10^{-31} \text{ m}^4 \text{ s}^{-1}$ and $r_{\max} = 2.25 \text{ } \mu\text{m}$.

From the porosity level of the anodes, which is about 40%, we can derive two estimations for r_{\max} . Assuming that for each particle the maximum available space for growth, i.e. the pore volume, is equal, we can calculate the pore volume V_p for the mean particle radius. Adding this value to the volume of a sphere with radius r_1 we finally have the maximum particle volume which corresponds to a sphere radius of $r_{\max} = 1.82r_m(0) = 1.82 \text{ } \mu\text{m}$. If we assume that at a porosity level of 40% the large particles have the pore volume of both large and small particles (each with identical volume fraction) for growth we find a maximum particle radius of $r_{\max} = 2.32r_m = 2.32 \text{ } \mu\text{m}$. The actual found value is close to the larger value.

From the parameter A we can calculate the surface diffusion coefficient. The following values for the other parameters appearing in A were used: $\gamma = 1.9 \text{ J/m}^2$ [14], $\Omega = 1.09 \times 10^{-29} \text{ m}^3$, and δ_s was approximated by the interatomic spacing ($2.5 \times 10^{-10} \text{ m}$). The resultant surface diffusion coefficient is $1.3 \times 10^{-12} \text{ m}^2/\text{s}$.

Additionally, the particle size distribution of a functional anode layer with a thickness of $5 \text{ } \mu\text{m}$ was measured after operation at 800 °C under H₂/3%H₂O/air gas and at a current density of 300 mA/cm². The Ni particle radius after 100 h of operation was 0.72 μm , after 2100 h of operation 0.79 μm . From these two values a diffusion coefficient of $1.3 \times 10^{-13} \text{ m}^2/\text{s}$ was calculated using $\beta = 0.75$ and a value for r_{\max} of 1.62 μm . This value corresponds to a linear reduction of the previous r_{\max} value according to the lower initial particle radius.

In Fig. 4 these values are plotted together with literature results of the surface diffusion coefficient. The determined values are below the relatively large scattering band of literature data. There might be at least two reasons for this deviation.

First of all the two particle model is, of course, a rather rough description of the complex microstruc-

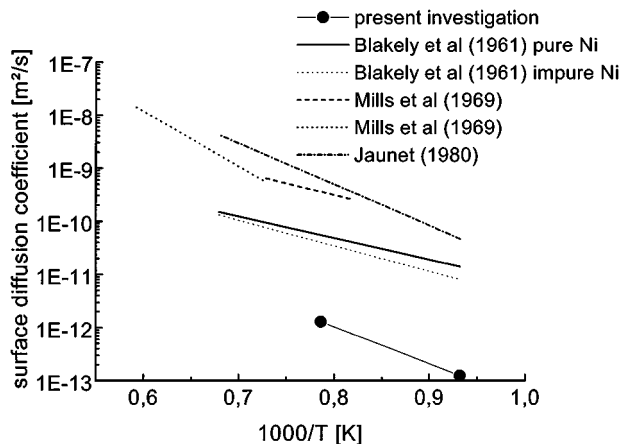


Figure 4 Comparison of the surface diffusion coefficient in Nickel found in literature [15] with the values obtained by a fit of (13) to the results of particle growth in SOFC anodes at 800°C and 1000°C.

ture of an SOFC anode (s. Fig. 2). So the hindrance of particle growth by the reduced “free” pore volume is incorporated into the model by a first order approximation (Equation 11). A more pronounced reduction of the particle growth rate by this effect would increase the surface diffusion coefficient.

A second possible reason for a reduction of the surface diffusion coefficient in our investigation can be the effect of surface contamination. A comparison of the results of Blakely for pure and impure (about 1 wt. % impurities) nickel given in Fig. 4 shows a reduction of the surface diffusion coefficient for impure nickel.

It should be noted that the slope of the two data points gives an activation energy of 1.4 eV, which is in the range of activation energies found in literature.

With the determined parameters also predictions for longer operation times are possible. For example, a 23% growth of the Ni particles in the functional layer is predicted by the model after 10000 h of operation at 800 °C.

4. Conclusions

A model for the nickel particle growth in SOFC anodes was developed. This model contains three parameters which can be all estimated from features of the used materials.

One parameter is related to the width of the particle size distribution and was determined directly from the experimentally found distributions. The second parameter is the maximum radius up to which the particles can grow. The value found by fitting the theoretical growth law to the experimental data is well in the range of reasonable values estimated from the porosity level of the anode.

From the third parameter the surface diffusion coefficient was determined to be $1.3 \times 10^{-12} \text{ m}^2/\text{s}$. This value is somewhat low compared to literature results. This might be due to some simplifications in the model and a possible surface contamination of the nickel particles.

Finally, we would like to emphasise that the applied model is able to describe the growth of nickel particles in SOFC anodes in a convincing way and that, to a certain extent, a prediction of growth rates for different

microstructures or different temperatures seems to be possible.

References

1. N. Q. MINH, *J. Amer. Ceram. Soc.* **76**(5) (1993) 563.
2. H. P. BUCHKREMER, U. DIEKMANN, L. G. J. DE HAART, H. KABS, U. STIMMING and D. STÖVER, in *Electrochemical Proceedings 97-18*, edited by U. Stimming, S. C. Singhal, H. Tagawa and W. Lehnert (The Electrochemical Society, Pennington, New Jersey, 1997) p. 160.
3. A. MÜLLER, A. WEBER, A. KRÜGEL, D. GERTHSEN and E. IVERS-TIFFÉ, in *Proc. of the Werkstoffwoche 98*, edited by A. Kranzmann and U. Gramberg (Wiley-VCH Verlag GmbH, Weinheim, 1999) Vol. 3, p. 171.
4. A. NAOUMIDIS, A. GUPTA, H. HOVEN, TH. KLOIDT, D. SIMWONIS and F. TIETZ, in *Proceedings of the 10th IEA Workshop on SOFCs, Materials and Processes*, edited by A. J. McEvoy and K. Nisancioglu (Inter. Energy Agency, 1997) Vol. 1, p. 119.
5. J. ABEL, A. A. KORNY SHEV and W. LEHNERT, **144**(12) (1997) 4253.
6. A. IOSELEVICH, A. A. KORNY SHEV and W. LEHNERT, *J. Electrochem. Soc.* **144**(9) (1997) 3010.
7. J. PAN, H. LE, S. KUCHERENKO and J. A. YEOMANS, *Acta Mater.* **46**(13) (1998) 4671.
8. G. C. KUCZYNSKI, *J. Appl. Phys.* **21** (1950) 632.
9. P. W. VOORHEES, *Journal of Statistical Physics* **38**(1/2) (1985) 231.
10. W. D. KINGERY and B. FRANCOIS, in "Sintering and Related Phenomena," edited by G. C. Kuczynski *et al.* (Gordon and Breach, New York, 1967) p. 471.
11. H. P. BUCHKREMER, U. DIEKMANN and D. STÖVER, *Proc. 2nd Europ. SOFC Forum 1996*, edited by B. Thostensen, (U. Bossel, Morgenacherstrasse 2F, CH-5452, Oberrohrdorf, Switzerland, 1996) p. 221.
12. M. I. MENDELSON, *J. Amer. Ceram. Soc.* **52**(8) (1969) 443.
13. D. SIMWONIS, PhD thesis, Ruhr-University Bochum, 1999.
14. J. M. BLAKELY and H. MYKURA, *Acta Metall.* **9** (1961) 23.
15. LANDOLT-BÖRNSTEIN, in "Diffusion in Solid Metals and Alloys," Volume 26, edited by H. Mehrer (Springer-Verlag, Berlin Heidelberg, 1990). Ch. 13: Surface Diffusion in Metals by H. P. Bonzel.

*Received 19 April 2000
and accepted 27 June 2000*